Pitch-angle Redistribution of Beam Ion Losses caused by Alfvén Instabilities in Sub-Cyclotron Frequency Range on the Mega Amp Spherical Tokamak Upgrade

J. F. Rivero-Rodriguez[1,2], S. E. Sharapov[1], L. Velarde[3], H.J.C. Oliver[1], K. G. McClements[1], M. Dreval[4], M. Fitzgerald[1], N. Crocker[5], J. Galdón-Quiroga[6], M. García-Muñoz[6], C. Michael[5], E. Viezzer[6], the EUROfusion Tokamak Exploitation Team and the MAST Upgrade Team

[1]*United Kingdom Atomic Energy Authority, Culham Campus, Abingdon, Oxfordshire OX14 3DB, United Kingdom*

[2]*Departamento de Ingeniería Mecánica y Fabricación, Escuela Técnica Superior de Ingeniería, Universidad de Sevilla, 41092 Sevilla, España*

[3]*Departamento de Ingeniería Energética, Escuela Técnica Superior de Ingeniería, Universidad de Sevilla, 41092 Sevilla, España*

[4]*Institute of Plasma Physics, National Science Center, Kharkov Institute of Physics and Technology, 61108 Kharkov, Ukraine*

[5]*Department of Physics and Astronomy, University of California, Los Angeles, CA90095, United States of America*

[6]*Departamento de Física Atómica, Molecular y Nuclear, Facultad de Física, Universidad de Sevilla, 41012 Sevilla, España*

Abstract Dedicated experiments were conducted on Alfvénic instabilities in the ion sub-cyclotron frequency range excited via Doppler-shifted ion-cyclotron-resonances by energetic beam ions in the MAST-Upgrade tokamak. Losses of the energetic ions associated with plasma instabilities were measured with a scintillator-type fast-ion lost detector (FILD), which provided a 2D image of the losses as functions of their pitch angle and energy. The data acquisition of the FILD allowed, for the first time, detection of fast-ion losses at frequencies up to half the ion cyclotron frequency. This made it possible to identify the source of the losses as global Alfvén eigenmodes (GAEs), excited via fast-ion cyclotron resonances. The Doppler-shifted cyclotron resonance interaction with counter-propagating GAE results mainly in redistribution of the fast ions in pitch angle. Linear modelling indicates that the wave-particle energy transfer leads to changes in the pitch angle that are proportionally larger than the net energy lost by the fast ions. The results concerning the pitch-angle redistribution indicate that neutral beam current drive in future magnetically confined fusion devices could be significantly degraded by Alfvenic modes in the ion-cyclotron range.

Introduction. Interactions of shear Alfvén and compressional Alfvén waves with energetic ions via Doppler-shifted ion-cyclotron-resonances is a fundamental topic of interest for magnetic nuclear fusion [1-7], laboratory [8-11] and space plasmas [12-14]. The similarities between these plasma phenomena provide an opportunity to study space plasmas effects in the laboratory, while the observation of large-scale space plasmas provide inspiration and context. The key issues to be studied in the physics of Doppler-shifted ion-cyclotron resonances are the wave-particle power transfer and its effect on the temporal evolution of the energetic ions' kinetic energy and magnetic moment. Such an ion-cyclotron interaction with electromagnetic waves has been proposed to explain the accelerated proton distributions measured near Jupiter's ionosphere [12] and enhanced heating in the solar wind [14]. The redistribution associated with the cyclotron resonances have been experimentally observed in the large plasma device (LAPD) [8, 9] by determining the properties of beam ions in the presence of well-controlled Alfvén waves launched with an external antenna. Such a redistribution was leveraged in JET, where J.P. Graves et al. used ion-cyclotron resonance heating to tune the fast-ion distribution and control the onset of deleterious magneto-hydro-dynamic (MHD) instabilities [7]. A similar approach has been considered to depopulate Earth's radiation belts of energetic protons by using satellite-launched waves to scatter protons in the Solar wind [11]. However, energetic ions themselves may excite Alfvén cyclotron instabilities if they have the sources of free energy associated with a bump-on-tail in the energy distribution and/or anisotropy [1,2]. In such cases a nonlinear description of the coupled wave-particle system is used for assessing the saturation amplitude of the Alfvén wave together with the fast-ion relaxation. The relaxation of the fast-ion distribution in velocity space can also cause some important physics effects in magnetically confined fusion: In the National Spherical Torus Experiment (NSTX), the excitation of many compressional Alfvén eigenmodes (CAEs) in the sub-cyclotron frequency range, followed by the fast-ion diffusion in velocity space,

transferred wave energy to thermal ions, causing anomalous heating [3]. Also, nonlinear simulations have shown that counter-current propagating global Alfvén eigenmodes (GAEs) in NSTX can redistribute beam energetic ions, causing changes in the fast ion's perpendicular and parallel energies that are several times larger than the total particle energy change [4]. This leads mainly to a fast-ion redistribution in pitch angle that flattens the fast-ion profiles. Such a fast-ion redistribution is a key issue in magnetic nuclear fusion. Fast-ion redistribution induced by Alfvén eigenmodes have been observed to eject fast ions onto the tokamak's wall, increasing the heat load on plasma facing components [15-20]. Also, fast-ion redistribution can limit the effectiveness of neutral beam current drive (NBCD) in future burning plasmas [5]. Moreover, the beam injection energies required in future burning plasmas to penetrate the dense plasma core will lead to super-Alfvenic fast ions, - i.e. ions with speeds above the Alfvén speed -, that will likely excite Alfvenic modes in the ion cyclotron range. Therefore, characterising the fast-ion redistribution caused by Alfvén modes in the ion cyclotron range becomes necessary to quantify the heat load on plasma facing components and to assess the feasibility of NBCD on future fusion devices.

In this Letter we present measurements of lost fast ion's pitch-angle redistribution induced by Alfvén eigenmodes close to half the ion-cyclotron frequency, measured for the first time at the Mega Amp Spherical Tokamak Upgrade (MAST-U). Detailed simulations identify the Alfvén modes as GAEs close to minima and maxima of the Alfvén continuum [6]. The observed pitch-angle redistribution agrees with an ion-cyclotron resonant wave-particle interaction where the fast ions transfer energy to the Alfvén wave.

The Experiment. MAST-U is a low aspect ratio tokamak with typical major and minor radii of 0.8 m and 0.5 m, respectively. The on-axis neutral beam injector (NBI), - with a tangency radius of 0.7 m and injecting horizontally at the machine midplane -, and the off-axis NBI, - with a tangency radius of 0.8 m and injecting

horizontally 0.65 m above the machine midplane -, provide the only confined fast-ion population in MAST-U. So far, the plasma current is counter-clockwise as seen from above and the toroidal magnetic field is clockwise in all MAST-U experiments. To detect electromagnetic fluctuations, an outboard Mirnov array for high frequency acquisition coils, digitised up to a 10 MHz sampling rate, are used, making it possible to perform measurements up to 5 MHz [21]. To determine electron density and electron temperature profiles, the Thomson scattering diagnostic [22] with high temporal resolution (33 ms) is employed, and a motional Stark effect (MSE) diagnostic is used for measuring the magnetic field pitch [23]. Fast-ion losses are directly measured with a scintillator-based Fast-Ion Loss Detector (FILD) [24-26]. The FILD data make it possible to infer the velocity space of the fast-ion losses, i.e., Larmor radius ($\rho_L = (mv_\perp)/(qB)$) and pitch angle ($\lambda = \cos^{-1}(-v_\parallel/\mathrm{v})$); where m and q are the mass and charge of the measured fast ion; B is the local magnetic field; $v_{//}$ and $v_\perp$ are the velocity components parallel and perpendicular to the magnetic field and v is the total velocity. λ is defined positive for fast ions moving in the direction of the plasma current. FILD detects only fast-ion losses with positive pitch angles, meaning particles moving in the direction of the plasma current and the beam injection, and opposite to the magnetic field. The fast-ion loss fluctuation is measured with a maximum sampling frequency of 4 MHz. Therefore, the Nyquist frequency of the FILD measurements is 2 MHz.

The MAST-U FILD routinely measures fast-ion losses coherent with bursting modes with frequencies in the MHz range excited by on-axis NBI. For simplicity, two types of discharges are considered here, one with higher plasma current and the waves propagating co-beam, and the other one with lower plasma current and the waves propagating counter-beam. In the experiment, deuterium (D) with maximum energy E_{max} = 63 keV is injected into D plasma with the on-axis beam thus generating a D beam fast-ion distribution function with maximum velocity of $V_{max} \cong 2.5 \cdot 10^3$ km/s, which is the only confined fast-ion population in MAST-U. The ratio of beam velocity to Alfvén velocity was in the range between 1.76 and 2.25, meaning that

the fast-ion distributions were super-Alfvénic. Figure 1 shows the main waveforms of example MAST-U discharges of the two types. The MAST-U discharges operated predominantly in H-mode, characterized by the consistent presence throughout the experiment of type-III ELMs, which are evidenced by the rapid sequence of spikes in the D-α emission (figure 1(c)), and sawtooth instabilities, which are observed as cyclic drops in the neutron rate (figure 1(e)) [27].

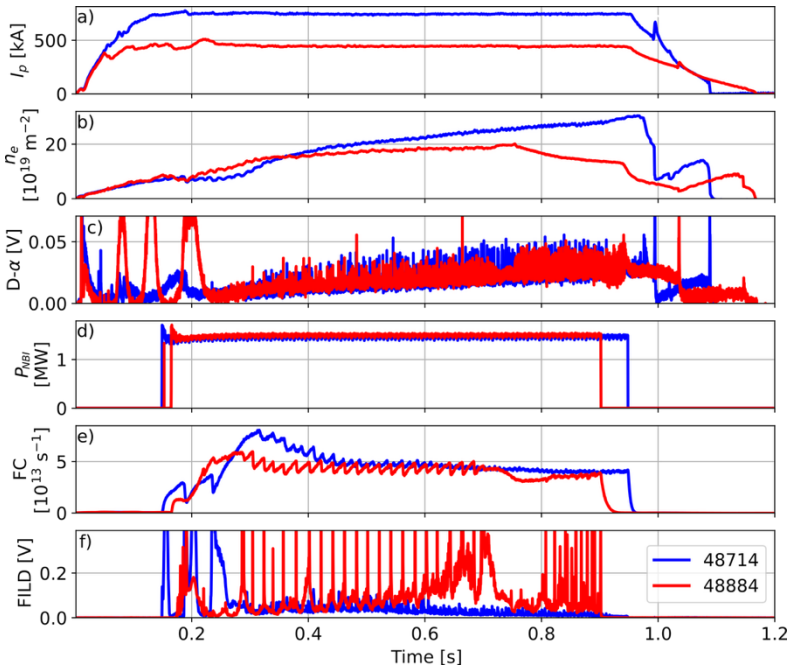

FIG.1. Time evolution of MAST-U discharges, #48714 (blue) and #48884 (red). From top to bottom, plasma current, line-integrated density, D-α emission, on-axis beam injected power, neutron rate measured with a fission chamber (FC) and fast-ion losses measured with FILD.

Discharge #48714 has toroidal field at the magnetic axis $B_0 = 0.64$ T and plasma current $I_p = 750$ kA. The relatively high plasma current improves the confinement of fast-ion drift orbits. The Mirnov coils detect beam-driven modes between 1.6 MHz and 2.4 MHz, as shown in figure 2(a). This is between 0.3 and 0.5 times the beam cyclotron frequency at the magnetic axis (4.9 MHz). The modes are interrupted by sawtooth crashes that reduce the radial gradient of the fast-ion profile, and the modes reappear when the fast-ion gradient is recovered. The modes propagate counter-clockwise as seen from above, in the direction of the current and

the beam injection, which corresponds to positive toroidal mode numbers ($n > 0$) in figure 2(a). The modes appear in frequency sidebands, with toroidal mode numbers $n = 5 - 13$. Modes with increasing n are separated 10 kHz from each other, while modes with the same n are separated around 100 kHz from each other. The fast-ion losses are measured with FILD, which has Nyquist frequency of 2 MHz, so figure 2(b) shows some aliased frequencies up to 520 ms. The measured losses on FILD correlate with the modes from figure 2(a), and they are mostly coherent with $n = 7, 9$ in the lower frequency band and $n = 9, 11$ in the upper band. Thus, MAST-U discharge #48714 reveals interactions between lost fast ions and co-propagating modes with frequencies of around half the ion-cyclotron frequency.

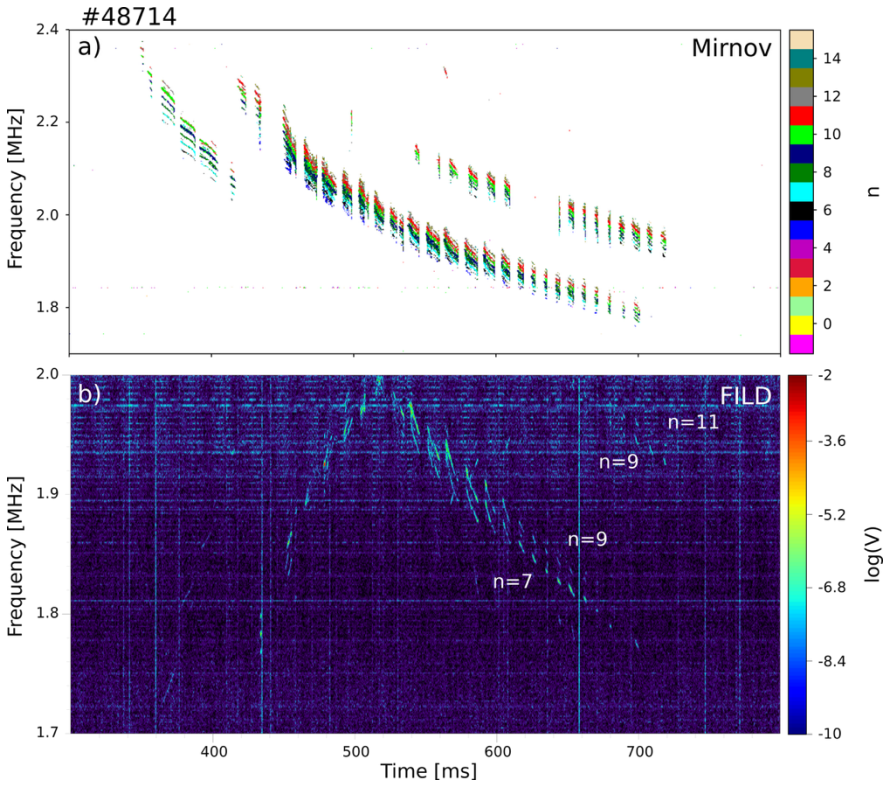

FIG. 2. MAST-U shot #48714. (a) Spectrograms of the magnetic perturbation measured by the Mirnov coils, with toroidal mode numbers shown in colours. (b) Fast-ion losses measured by FILD.

In contrast, shot #48884 has $B_0 = 0.5$ T and $I_p = 450$ kA, increasing the widths of fast-ion orbits and reducing their confinement. Thus, the FILD signal is higher and more sensitive to the detection of fast-ion redistribution. For instance, it can be

observed in figure 1(f) that sawtooth-induced losses are high in the 450 kA shot but hardly observed in the 750 kA shot. The beam-driven modes now appear in the frequency range of 1.2 – 2 MHz in a similar pattern as shot #48714, as observed in figure 3(a). Furthermore, the frequency of the modes is again between 0.3 and 0.5 times the beam cyclotron frequency at the magnetic axis (3.8 MHz). However, in shot #48884 the toroidal mode numbers are negative, between $n = -5$ and $n = -10$, meaning that the modes propagate counter-current and counter-beam. The modes appear in frequency sidebands as in shot #48714 but in this case the absolute value of the toroidal number n decreases as frequency rises. Fast-ion losses correlated with counter-current modes can be seen in the frequency range of 1.5 to 2 MHz, as shown in figure 3(b). These losses are coherent with $n = -6$ and $n = -7$ modes. Discharge #48884 thus reveals the interactions between lost fast ions and counter-propagating modes in the range of half the ion-cyclotron frequency. It can be observed that, in both #48714 and #48884, the fast-ion losses are not coherent with all the detected modes but only to specific frequencies and mode numbers, suggesting that specific resonance conditions between the fast-ion orbits and the waves need to be met for the modulation to occur.

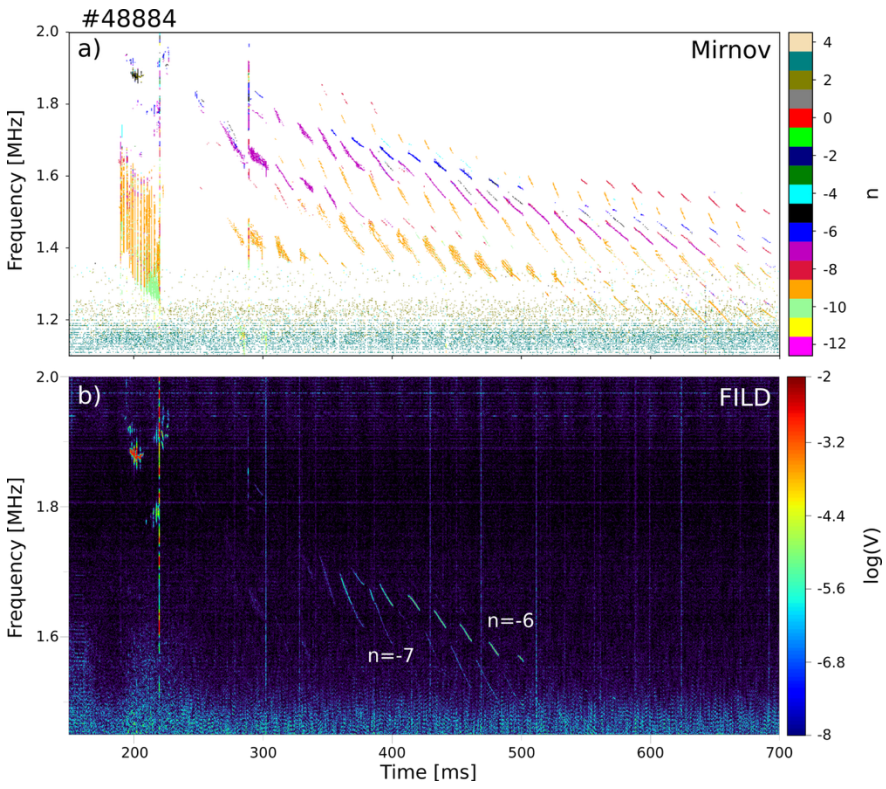

FIG. 3. MAST-U shot #48884. (a) Spectrograms of the magnetic perturbation measured by the Mirnov coils, with toroidal mode numbers shown in colours. (b) Fast-ion losses measured by FILD.

Pitch-angle redistribution of the losses. The velocity space of the losses measured by FILD in each discharge are processed with the FILDSIM code [28, 29] to plot the losses in a Cartesian energy/pitch-angle grid, as shown in figure 4(a) and 4(b). In both shots, the distribution in energy is centred on a value close to the NBI injection energy, 63 keV. Given the finite resolution of the diagnostic in energy, this likely corresponds to a monoenergetic fast-ion distribution reaching the FILD probe [30, 31]. In contrast, the pitch-angle resolution is significantly higher. The distribution in pitch angle shows a single peak at approximately 57° in shot #48714, while the distribution in #48884 is split in two local maxima between 55° and 60°. Nevertheless, the pitch angle of the losses is similar in both shots.

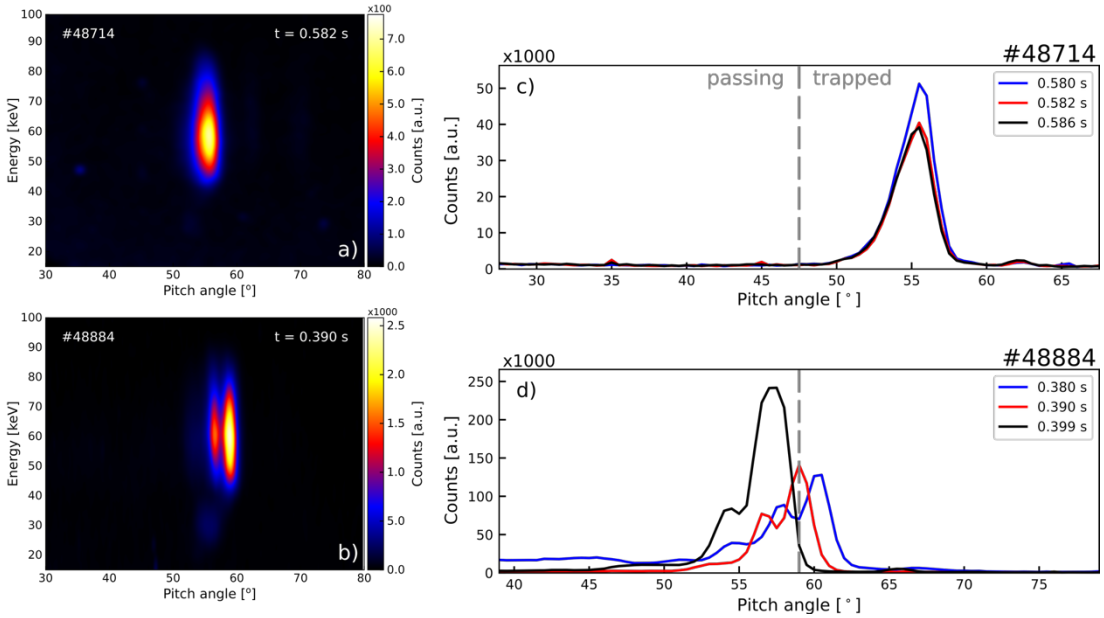

FIG. 4. Fast-ion losses measured with the MAST-U FILD measured in shot #48714 (a) and #48884 (b), remapped into velocity-space coordinates. Note the difference in the colour scale. Pitch-angle distribution of the fast-ion losses measured in shots #48714 (c) and #48884 (d) during the

excitation of high-frequency modes, integrated over all gyroradii. The grey vertical lines mark the trapped-passing boundary pitch angle.

Figure 4(c) and 4(d) show the temporal evolution of the pitch-angle distribution in pulses #48714 and #48884, respectively, between two sawtooth crashes and during the excitation of high-frequency modes. In #48714, the losses are well above the trapped-passing boundary pitch angle, marked by the grey dashed line. Comparison of 3 frames integrated over all giroradii in figure 5(c) shows that the losses are nearly constant in pitch angle, indicating that pitch-angle redistribution by co-current modes is small. In contrast, the two peaks in the pitch-angle distribution of pulse #48884 at t = 0.380 s (blue) are above and below the trapped-passing boundary pitch angle, respectively. The pitch angle of lost ions evolves in time significantly towards lower values. During the temporal evolution of the pitch angle, the trapped lost ion distribution crosses the trapped-passing boundary, modifying the orbit topology of the fast-ion losses from trapped to passing. This leads to a factor 2 increase in the amplitude of the FILD signal. The pitch-angle descent occurs when high-frequency losses are coherent with $n = -6$ modes, as can be observed in figure 5, indicating a strong pitch-angle redistribution induced by counter-beam modes. The descent is only interrupted by the burst of losses during the sawtooth crashes. This causes a cyclic evolution of the pitch angle, where the $n = -6$ mode reduces it until the sawtooth crash restores it to its original value.

The cyclic evolution of the fast-ion pitch angle observed in figure 5 is not correlated with changes in the safety factor, q, through the sawtooth cycle. On the one hand, FILDSIM corrects any changes in the local magnetic field pitch to calculate the lost fast-ions pitch angle. On the other hand, MSE measurements show that even though this cycle is observed in the safety factor at the magnetic axis, q_0, which is not explored by the lost fast-ion orbits, the rest of the q-profile does not reveal any cyclic evolution that can explain the pitch-angle changes.

Note that while figures 2 and 3 showed fast-ion loss fluctuations at frequencies coherent with Alfvén waves, figure 4 and 5 shows the slow temporal evolution of the fast-ion loss velocity space. The former suggests resonance interactions between the fast-ion orbits and the waves, the latter indicates a slow pitch-angle redistribution induced by such an interaction.

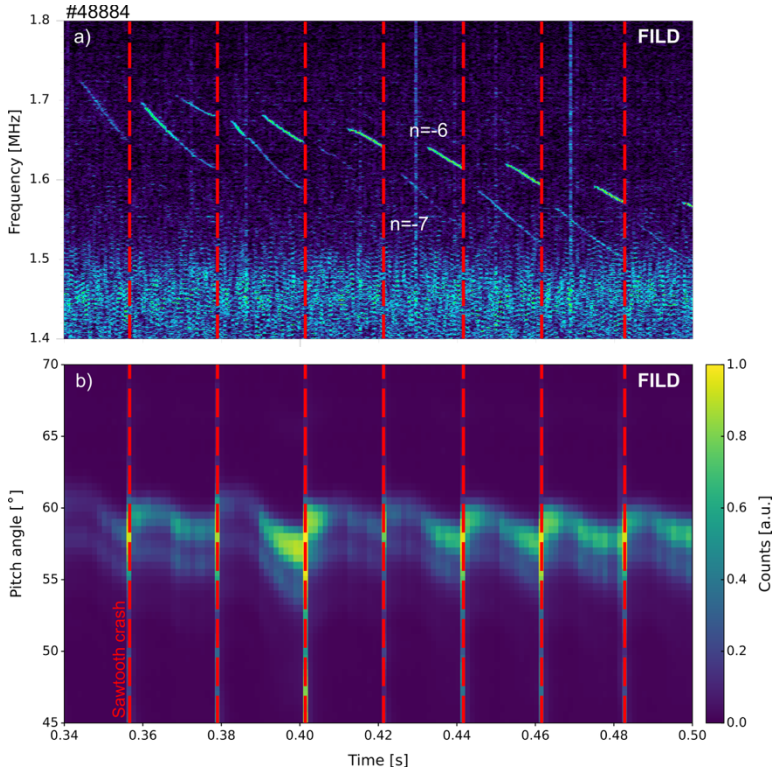

FIG. 5. (a) Spectrogram and (b) pitch angle of the fast-ion losses in MAST-U discharge #48884. The red vertical lines mark each sawtooth crash.

Wave-particle interaction. To determine the role of the $n = -6$ wave in the fast-ion pitch-angle redistribution, full gyro-orbit calculations of linear wave-particle interactions are carried out with the perturbative code HALO [32]. First, the magnetic equilibrium of MAST-U discharge #48884 is reconstructed with EFIT++, constrained with magnetics data and the magnetic field pitch measured with MSE. The shear Alfvén continuum of MAST-U discharge #48884 at $t = 0.365$ s for $n = -6$ is calculated with the CSCAS code [33], solving the ideal, incompressible MHD

equations [34]. The continuum is shown in figure 6(a) between frequencies 6 and 9 v_{A0}/R_0, being $v_{A0} = 1.3{\cdot}10^3$ km/s the Alfvén speed at the magnetic axis, $R_0 =$ 1.0 m. The Alfvén continuum shows a maximum near 8.25 v_{A0}/R_0, where a potential well localises shear Alfven waves, creating a GAE. Among all the eigenmodes obtained with the MISHKA stability code [35] near this maximum, the mode with the highest growth rate (γ/ω=1.53 %) is shown in figure 6(b). The mode has radial number l = 0, and poloidal mode numbers m = 10, 11, 12, 13. The frequency of this mode, marked by the dashed red line in figure 6(a), is 8.27 v_{A0}/R_0. This corresponds to 1.66 MHz in laboratory reference (accounting for the plasma rotation) which is close to the experimental frequency of the $n = -6$ mode in pulse #48884 (1.68 MHz). Thus, the counter-propagating wave that modulates the fast-ion losses in MAST-U is confirmed to be a counter-propagating GAE formed just above the maxima of the Alfvén continuum, usually referred to as non-conventional GAE [36, 37].

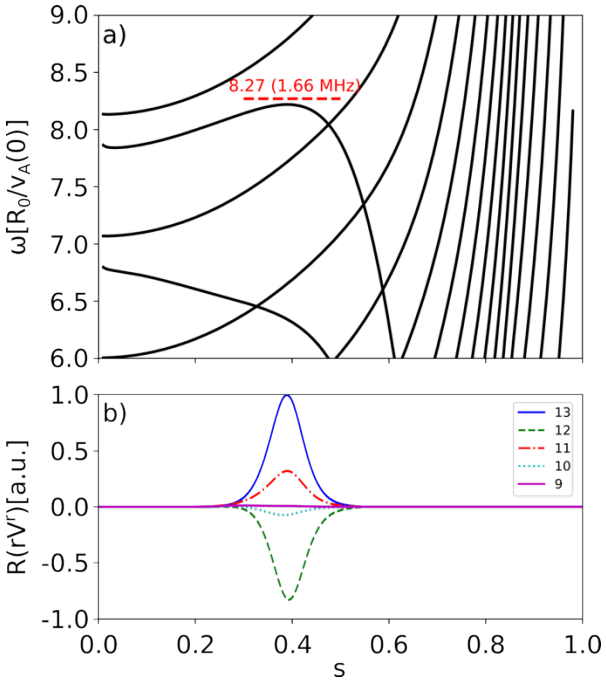

FIG. 6. (a) Alfvén continuum structure of MAST-U shot #48884 at t = 0.365 s for n = -6. The frequency of the most unstable mode found with MISHKA near the local maximum is shown in red. (b) Plasma potential Φ of the most unstable n = -6 GAE solved with MISHKA.

HALO computes the power transfer between the wave and the fast ions as the work done by the fast ions on the wave, and vice versa, for the fast-ion orbits that satisfy the ion-cyclotron resonance condition ($\omega = n\bar{\omega}_\phi + p\bar{\omega}_\theta + l\bar{\omega}_{ci}$), where ω is the wave frequency, $\bar{\omega}_\phi$ and $\bar{\omega}_\theta$ are the averaged toroidal and poloidal orbit frequencies, $\bar{\omega}_{ci}$ is the averaged ion-cyclotron frequency, and p and l are integers. The simulation uses the mode structure estimated by MISHKA, and a distribution of 56 million markers that mimic the steady-state fast-ion distribution in #48884 computed using the full orbit code LOCUST-GPU [38, 39]. LOCUST followed a sample of beam markers generated by TRANSP/NUBEAM [40, 41] at the time of ionisation until thermalisation or loss to the first wall. The distribution function computed by LOCUST is sufficiently smooth to use for stability studies without smoothing or splining [42] due to the large number of particles followed. The beam distribution function and eigenmode are used to compute the power transfer using the HALO code. Figure 7 shows a histogram of the linear power transfer between the wave and the steady-state fast-ion distribution over the constants of motion in unperturbed fields (i.e. normalised toroidal canonical momentum, $P_\phi = mRv_\phi + Ze\psi$, and normalised magnetic moment, $\Lambda = \frac{\mu B_0}{E}$). Energy transferred from the wave to the fast ions (wave damping) is shown in blue, and energy transferred from the fast ions to the wave (wave drive) is shown in red. The colour scale is normalised to the maximum energy transferred to the wave. The losses detected experimentally by FILD in #48884 (peaks in figure 4(d)) are marked with crosses in the figure. It can be observed that most of the wave drive comes from co-passing orbits ($P_\phi = [0.2, 0.7],\ \Lambda < 0.8$), meaning that the observed losses, even though they interact with the wave, are not the main responsible for driving the GAE unstable. At the region of the observed losses the power transferred to the wave is two orders of magnitude lower than the maximum energy transferred to the wave. Therefore, the results indicate that even though the fast-ion losses are most likely not the main responsible for the wave drive, they are affected by the wave-particle resonant interaction, losing net energy to the wave.

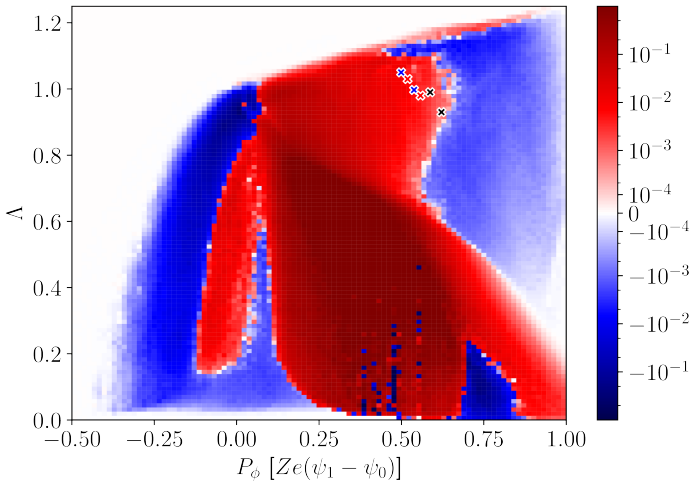

FIG. 7. Histogram of power transferred from the wave to the fast ions (blue) and from the fast ions to the wave (red). The colour scales are normalised to the maximum energy transferred to the wave. The losses measured in shot #48884 are marked by blue (t = 380 ms), red (t = 390 ms) and black (t = 399 ms) crosses.

Correlation between experimental observations and numerical results. The pitch-angle redistribution observed experimentally agrees with the energy transfer modelled by HALO. In an ion-cyclotron resonance, two constants of motion are conserved, $C_1 = E - \frac{\omega}{\omega_{ci}} B_0\, \mu$ and $C_2 = E - \frac{\omega}{n} P_\phi$. The conservation of C_1 implies that energy exchanged with a sub-cyclotron wave results in a change in perpendicular energy ($\Delta E_\perp \approx B_0 \Delta\mu$) that is several times the total energy change ($\Delta E = \frac{\omega}{\omega_{ci}} \Delta E_\perp$), so it mainly leads to a redistribution in pitch angle [4]. Therefore, a loss in total energy (as predicted by the modelling) will result in a decrease in pitch-angle (as observed experimentally). In MAST-U shot #48884, where $\frac{\omega}{\omega_{ci}} = 0.43$, the fast-ion distribution observed in figure 4(d) evolves from a pitch angle of 60º to 57º. Assuming an initial energy of 63 keV, by conservation of C_1, a reduction of 3º in pitch angle corresponds to 1.4 keV of total energy loss. While the pitch-angle redistribution is clearly observed experimentally, the reason why the energy loss cannot be distinguished in the FILD data is because it falls below the diagnostic

energy resolution limit (~10 keV) [30]. In contrast, the observed pitch-angle change is indeed above the pitch-angle resolution limit (0.6°).

Discussion. This Letter has presented the first direct measurements of fast-ion pitch-angle redistribution caused by sub-cyclotron Global Alfvén Eigenmodes (GAEs). Dedicated experiments on MAST-U employed a scintillator-based Fast-Ion Loss Detector (FILD), which provided velocity-space measurements of beam ion losses up to half the beam ion cyclotron frequency. This enabled a detailed assessment of losses associated with bursting Alfvén eigenmodes excited by the on-axis NBI observed at frequencies between 0.3 and 0.5 times the ion cyclotron frequency. The modes were identified as GAEs propagating in both co- and counter-current directions [6]. In contrast to co-current GAEs, which showed minor pitch-angle changes, counter-current GAEs observed in lower plasma current discharges led to a significant evolution of the lost ion distribution towards lower pitch angles. This evolution implied trapped orbits crossing the trapped-passing boundary, increasing the amplitude of the losses.

Full gyro-orbit simulations performed with the perturbative HALO code indicate that the detected fast-ion losses transfer net energy to the wave via ion-cyclotron resonance, even though they are likely not the primary drivers of the GAE instability. Instead, they are modulated by the wave's presence, transferring energy to it, which leads to significant changes in their orbits. By conservation of constants of motion in an ion-cyclotron resonant interaction, the results show that such an interaction will mainly lead to a redistribution in pitch angle, as observed experimentally.

These results are crucial for advancing the understanding of wave-particle interactions in magnetically confined fusion plasmas. The experimental evidence from MAST-U shows that ion-cyclotron resonance can lead to significant pitch-angle redistribution of super-Alfvénic fast ions. This confirms the results from previous nonlinear simulations in NSTX [4], which predicted pitch-angle

redistribution of the beam ions that drive counter-propagating GAEs. FILD probes a localised region of the fast-ion phase space, making it possible to observe the redistribution within it. However, it is very likely that the redistribution caused by counter-current GAEs affect a wider phase space of the fast-ion distribution, as indicated by the nonlinear simulations [4]. Given that negative ion beams in future devices like ITER and JT-60SA will generate anisotropic super-Alfvénic fast-ion distributions prone to driving GAEs and CAEs unstable, accurate modelling of pitch-angle redistribution will be essential for predicting and optimizing heating and current drive efficiency in these next-generation tokamaks. In particular, these results call for an urgent assessment of NBCD effectiveness in future burning plasmas, where pitch-angle redistribution can severely deteriorate it [5]. Furthermore, these findings contribute to a broader comprehension of analogous electromagnetic wave effects observed in space plasmas, such as the scattering of solar wind particles arriving at Earth's magnetosphere [11, 14] or the distribution of accelerated protons observed near Jupiter's ionosphere [12].

Acknowledgements. This work has been carried out within the framework of the EUROfusion Consortium, funded by the European Union via the Euratom Research and Training Programme (Grant Agreement No 101052200 — EUROfusion) and by the EPSRC [grant number EP/W006839/1]. To obtain further information on the data and models underlying this paper please contact PublicationsManager@ukaea.uk. Views and opinions expressed are however those of the authors only and do not necessarily reflect those of the European Union or the European Commission. Neither the European Union nor the European Commission can be held responsible for them. This research received funding from the VII Plan Propio de Investigacion de la Universidad de Sevilla. This research received funding from the Plan Andaluz de Investigación, Desarrollo e Innovación (PAIDI 2020, No. 003456/A02W), Consejería de Transformación Económica, Industria, Conocimiento y Universidades de la Junta de Andalucía. This project has

received funding from the European Research Council (ERC) under the European Union's Horizon 2020 research and innovation programme (Grant Agreement No. 805162).

References

[1] W.W. Heidbrink, Phys. Plasmas 15, 055501 (2008);

[2] S.E. Sharapov et al., Phys. Plasmas 21, 082501 (2014);

[3] D.A. Gates et al., Phys. Rev. Lett. 87, 205003 (2001);

[4] E.V. Belova et al., Phys. Plasmas 31, 092510 (2024);

[5] W.W. Heidbrink et al., Phys. Rev. Lett. 99, 245002 (2007);

[6] M.B. Dreval et al., Nucl. Fusion 65, 016043 (2025);

[7] J.P. Graves et al., Nat. Commun. 3, 624 (2012);

[8] Y. Zang et al., Phys. Plasmas 15, 102112 (2008);

[9] W. Gekelman et al., Phys. Plasmas 18, 055501 (2011);

[10] S.K.P. Tripathi et al., Phys. Rev. E 91, 013109 (2015);

[11] S. Vincena et al., Americal Physical Society Annual Meeting TO8.00006 (2019);

[12] G. Clark et al., Front. Astron. Space Sci. 10, 1-13 (2023);

[13] M.E. Koepke, Rev. Geophys. 46, 3 (2008);

[14] J.C. Kasper et al., Phys. Rev. Lett. 110, 091102 (2013);

[15] S.J. Zweben et al., Nucl. Fusion 31, 2219 (1991);

[16] M. García-Muñoz et al., Phys. Rev. Lett. 100, 055005 (2008);

[17] M. García-Muñoz et al., Phys. Rev. Lett. 104, 185002 (2010);

[18] M. Van Zeeland et al., Phys. Plasmas 18, 056114 (2011);

[19] X. Chen et al., Phys. Rev. Lett. 110, 065004 (2013);

[20] J. Galdon-Quiroga et al., Nucl. Fusion 58, 036005 (2018);

[21] M.J. Hole et al., Rev. Sci. Instrum. 80, 123507 (2009);

[22] R. Scannell et al., Rev. Sci. Instrum. 81, 10D520 (2010);

[23] N. J. Conway et al., Rev. Sci. Instrum. 81, 10D738 (2010);

[24] S.J. Zweben, Nucl. Fusion 29, 825 (1989);

[25] M. García-Muñoz et al., Rev. Sci. Instrum. 80, 053503 (2009);

[26] J.F. Rivero-Rodriguez et al., Rev. Sci. Instrum. 89, 10I112 (2018);

[27] J.F. Rivero-Rodriguez et al., Nucl. Fusion 64 086025 (2024);

[28] J. Galdon-Quiroga et al., Plasma Phys. Control. Fusion 60, 105005 (2018);

[29] Jose Rueda Rueda et al. JoseRuedaRueda/ScintSuite: v1.4.1. https://doi.org/10.5281/zenodo.16709806 (2025);

[30] L. Velarde et al., Plasma Phys. Control. Fusion 67, 015024 (2025);

[31] M Jimenez-Comez et al., Plasma Phys. Control. Fusion 67 125005 (2025);

[32] M. Fitzgerald et al., Comput. Phys. Commun. 252, 106773 (2020);

[33] G.T.A. Huysmans et al., Int. J. Mod. Phys. C 02, 371–6 (1991);

[34] W. Kerner et al., J. Comput. Phys. 142, 271 (1998);

[35] A.B. Mikhailovskii et al., Plasma Phys. Rep. 23, 841 (1997);

[36] N.N. Gorelenkov el al., Nucl. Fusion 50, 084012 (2010);

[37] N.N. Gorelenkov el al., Nucl. Fusion 54, 125001 (2014);

[38] R. Akers et al., 39th EPS Conf. and 16th Int. Congress on Plasma Physics (2012);

[39] S.H. Ward et al., Nucl. Fusion 61 086029 (2021);

[40] R.J. Goldston et al., J. Comput. Phys. 43, 61 (1981);

[41] A. Pankin et al., Commun. Comput. Phys. 159, 157 (2004);

[42] H.J.C. Oliver et al., Nucl. Fusion 63, 112008 (2023).